nature neuroscience

The representation of perceived angular size in human primary visual cortex

Scott O Murray[1], Huseyin Boyaci[2] & Daniel Kersten[2]

Two objects that project the same visual angle on the retina can appear to occupy very different proportions of the visual field if they are perceived to be at different distances. What happens to the retinotopic map in primary visual cortex (V1) during the perception of these size illusions? Here we show, using functional magnetic resonance imaging (fMRI), that the retinotopic representation of an object changes in accordance with its perceived angular size. A distant object that appears to occupy a larger portion of the visual field activates a larger area in V1 than an object of equal angular size that is perceived to be closer and smaller. These results demonstrate that the retinal size of an object and the depth information in a scene are combined early in the human visual system.

Differences in perceived distance can have a marked effect on estimations of object size[1–4]. Many well-known size illusions are based on this effect and they are often very compelling. For example, the moon illusion—the fact that the moon looks considerably larger on the horizon than it does at its zenith—is no less apparent despite knowing that its size remains constant through the sky[5–8]. Though size illusions can often be explained by principled size-depth relationships[1,2,6,9–12], they raise an important question regarding the organization of the human visual system. One of the most fundamental properties of human primary visual cortex (V1) is the precise mapping of visual angle subtense onto the cortex. What happens to this retinotopic map when our perceptions of angular size are dramatically changed owing to differences in perceived depth? While holding an object's physical angular size constant, we show that the spatial extent of activation in V1 changes according to the object's perceived angular size.

RESULTS

Behavioral measurements of the size illusion

We used a rendered three-dimensional (3D) scene of a hallway and walls to present objects (spheres) at either a close ('front') or far ('back') apparent depth (**Fig. 1a**). Behavioral measurements showed that subjects perceived the angular size (diameter) of the back sphere to be at least 17% larger (s.e.m. = 1.9%) than that of a front sphere of identical angular size ('angular size illusion'), a finding consistent with other studies showing that for a given angular size, distant objects appear to occupy more of the visual field than closer objects[2,3,10,11]. This effect was very robust and reliable over several measurement techniques (see **Supplementary Methods** online). Specifically, although the precise magnitude varied with different measurement techniques, the direction of the perceptual effect did not depend on whether the spheres were presented successively, simultaneously, briefly, for long durations or with added dynamic textures. For the perceptual estimates reported here, we used a method-of-adjustment technique (see Methods) that consistently estimated the smallest effect-size across subjects, giving us a lower bound on the estimated illusion size.

fMRI measurements of the size illusion

To localize differences in brain activity corresponding to the changes in perceived angular size, we performed an fMRI experiment using stimulus conditions similar to those in the behavioral experiment. The 3D background (hallway and walls) was always present and the spheres always had the same angular size (6.5° visual angle). To ensure a large fMRI signal, the spheres were rendered with a checkerboard texture that counterphase-flickered at 8 Hz. The front and back spheres were presented in successive 10-s blocks and separated by 10-s fixation periods with a fixation mark at the center of each sphere's future presentation position (**Fig. 1b**). Fixation was maintained at the centers of the spheres. During scanning, all subjects reported having a strong size illusion: the back sphere appeared to occupy a larger portion of the visual field than the front sphere. Regions of interest (ROIs) in V1 corresponding to five different eccentricities along the radius of, and extending beyond, the spheres were identified using standard retinotopic mapping procedures (refs. 13,14; **Fig. 2a–c**). Event-related signal averages for each subject were calculated with each location's (front versus back) own fixation periods serving as baseline (**Fig. 3**, middle column). The average response 6–10 s after presentation of a sphere served as a peak measurement for each ROI.

The fMRI response to the back (perceptually larger) sphere extended in eccentricity beyond the response to the front (perceptually smaller) sphere (**Fig. 3**, top row), despite the fact that both spheres occupied identical visual angles. In particular, the peak response for the third and fourth ROIs, which occupied the approximate boundary of the spheres,

[1]Department of Psychology, University of Washington, Box 351525, Seattle, Washington 98195, USA. [2]Department of Psychology, University of Minnesota, 75 East River Road, Minneapolis, Minnesota 55455, USA. Correspondence should be addressed to S.O.M. (somurray@u.washington.edu).

Received 1 November 2005; accepted 13 January 2006; published online 5 February 2006; doi:10.1038/nn1641

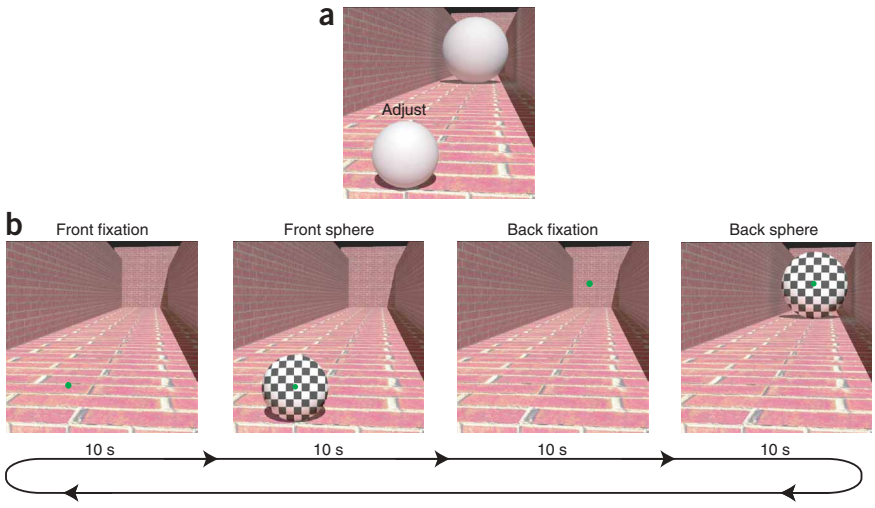

Figure 1 Stimulus for the behavioral and fMRI experiments. (**a**) In the behavioral experiment, subjects were asked to adjust the front sphere to match the angular size of the back sphere so that the two images of the spheres would overlap perfectly if they were moved to the same location on the screen. A larger-scale demonstration of the stimulus and size illusion is available at http://faculty.washington.edu/somurray/sizedemo.html. (**b**) A schematic of the experimental design used in the fMRI experiment. Subjects maintained fixation on a small green dot. The spheres were rendered with counterphase-flickering checkerboard patterns. Each condition was presented in succession for 10 s and then repeated five times in each scan.

was significantly higher for the back sphere than for the front sphere. To estimate the size of the fMRI effect, we calculated the average difference (see Methods) between the front and back peak response curves. The curve in response to the back sphere extended in eccentricity beyond that in response to the front sphere by an average eccentricity of 20% (maximum difference = 23%), which was approximately equivalent to the measured perceptual effect.

To compare the result obtained with a perceived difference in angular size to that obtained with an actual difference in angular size, two separate two-dimensional (2D) measurements were also performed where the 3D context (hallway and walls) was replaced with a uniform gray screen (**Fig. 3**, middle and bottom rows). The screen locations of checkerboard stimuli ('disks') were matched to the locations of the spheres in the 3D scene and, to approximately match the percept in the 3D scene, the top disk had a larger angular size than the bottom disk. The peak fMRI response in the same five ROIs depended on the angular size of the disk: activity in response to the larger disk extended in eccentricity beyond that in response to the smaller disk. The differences in response curves were similar for the 6.5° and 8.125° comparison (maximum difference = 25%, mean = 20%) and the 4.875° and 6.5° comparison (maximum difference = 25%, mean = 15%). Overall, the distribution of activity using the 2D disks with an actual difference in angular size closely resembled the response difference to the spheres in the 3D scene, which had only a perceptual difference in size.

An alternative way to characterize the fMRI effect in the 3D experiment is to estimate the absolute 2D eccentricities activated by the 3D stimuli. Specifically, we wanted to determine how many degrees of 2D visual angle in cortex were activated by the near and far 3D stimuli. To do this, we required a criterion for deciding at what point activation 'ends' in the cortex. We did this by determining a criterion in the 2D experiments (middle and bottom panels in **Fig. 3**) that matched the actual retinal size and then applying this criterion to the 3D data. We found that for the 6.5° conditions in the 2D experiments, the response curves matched the retinal size when the curves were at 22% of their maximum value. Applying this criterion to the 3D data revealed that the front and back spheres activated an area corresponding to 2.9° and 3.5° of cortex, respectively. Keeping in mind that the radius of the spheres was 3.25°, the front sphere activated a smaller absolute cortical area and the back sphere activated a larger absolute cortical area than did a 2D stimulus of equivalent size. We return to this point in the following control experiments.

Control experiments

Although there were small differences in background features surrounding the front and back spheres in the 3D scene, it is unlikely

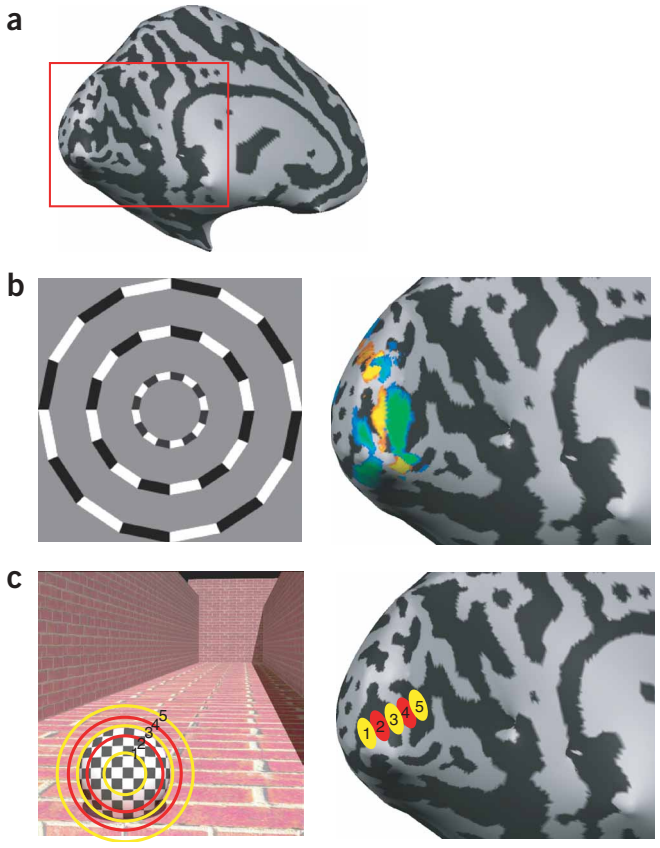

Figure 2 ROIs. fMRI data were analyzed in V1 in five adjacent ROIs of equal size extending along the eccentricity dimension. (**a**–**c**) In **a**, the area shown in greater detail in **b** and **c**. Counterphase-flickering annuli (**b**, left) were used at varying eccentricities to define the ROIs. The cortical area (**b**, right) activated by three such annuli that correspond to positions 1, 3 and 5 in **c**. The blue/green colormap represents responses to the inner annulus (leftward activation on the inflated cortical representation) and outer annulus (rightward activation on the inflated cortical representation). The red/yellow colormap represents responses to the middle annulus. (**c**) The five ROI positions and their approximate mapping onto the stimulus.

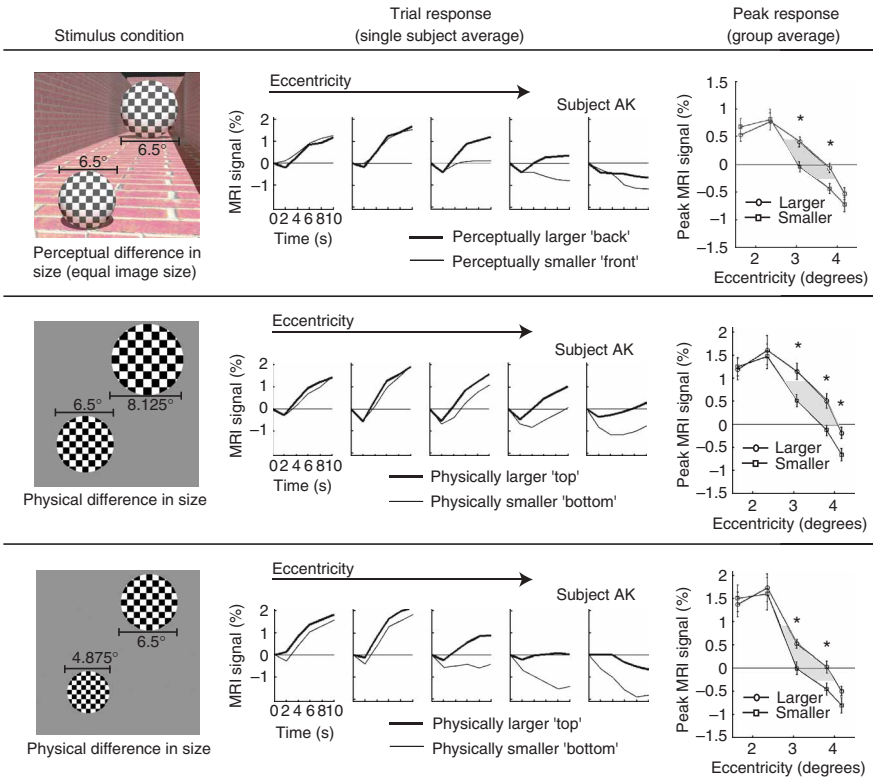

Figure 3 Imaging results. For each stimulus condition, event-related averages in V1 were calculated for each of five subjects (example subject, middle column), where time = 0 is the start of a checkerboard presentation. Peak measurements were averaged across hemispheres and subjects (right column). For both a perceptual difference in angular size (top row) and an actual difference in angular size (middle and bottom rows), activity for the larger stimulus extended in eccentricity beyond that for the smaller stimulus. The shaded region between the peak response curves (right column) shows the range over which differences in the curves were calculated (see main text and Methods). $*P < 0.05$. Error bars represent s.e.m.

that they contributed to the measured differences. The signals in response to the front and back spheres were measured with respect to fixation at each of those locations. Thus, for both the front and back spheres, the signal measured was with respect only to the addition of a sphere to the local background features (which were static and present during the fixation periods). However, there could have been differences caused by the relationship between the spheres and the local features in the scene. In particular, lighting differences in the renderings caused the contrast between the back sphere and its surround to be higher than that between the front sphere and its surround. To examine the effects of local contrast, we included a 2D condition that matched the mean luminance of the spheres and background in the 3D scene. We observed no differences in peak activity in response to the top (higher contrast) and bottom (lower contrast) disks (**Fig. 4a**).

An additional feature of the peak response curves for the 2D disks (**Fig. 4a**) is that they were at the midpoint between the front and back peak response curves measured with the 3D scene (dashed lines, **Fig. 4a**). That is, the response to the back sphere in the 3D scene extended beyond the response to an equivalently sized 2D disk, and the response to the front sphere was restricted to a smaller area than the response to an equivalently sized 2D disk. We drew the same conclusion from the estimates of the absolute 2D eccentricities activated by the 3D stimuli, as discussed in the previous section. We tested whether perception follows a similar symmetric pattern: does the back sphere appear to be larger and the front sphere appear to be smaller than an equivalent 2D disk? We used a matching paradigm where subjects adjusted a 2D disk located outside the 3D scene to match the size of the front and back spheres. We found that subjects reliably judged the angular size of a 2D disk to be intermediate between that of the front and back spheres (**Fig. 4b**). This symmetry in perception is consistent with the symmetry observed in the fMRI data.

Next, we used these behavioral measures to estimate the cortical area activated by the 3D stimuli. The front sphere appeared to be 0.91 times smaller than an equivalently sized 2D disk. Applying this behaviorally derived scale factor ($3.25^\circ \times 0.91$) gave an estimate (2.95°) of the 2D cortical area activated in response to the front sphere. Recall that in the previous section, based on the fMRI curves, our estimate of absolute 2D eccentricity activated by the front sphere was 2.90°. Thus, there was a high degree of correspondence between the behaviorally derived and fMRI-derived estimates. The behaviorally derived scale factor applied to the back sphere ($3.25^\circ \times 1.04 = 3.38^\circ$) was, again, close to our previous fMRI-derived estimate of 3.50°. Though the fMRI estimates were slightly larger, there was notable agreement between what was predicted from the direction and magnitude of the behavioral effect and what was measured with fMRI.

We performed a final control experiment that had two primary objectives. First, we wanted to minimize any differences of local stimulus features surrounding the front and back spheres; we achieved this by using a greatly simplified 3D scene (similar to the classic Ponzo illusion). The only depth cues were two lines with linear perspective and a small luminance gradient on an otherwise gray screen (**Fig. 4c**). Second, we wanted to investigate whether reducing the perceptual effect also reduced the fMRI effect. There was some evidence to suggest that there was a correlation between the strength of the perceptual effect across subjects and the size of the fMRI effect in the original experiment (see **Supplementary Data** online), but a different way to address this question is to use a stimulus configuration that is known to reduce the strength of the perceptual effect. As expected, the perceptual effect with the reduced depth cues was at least 16% smaller than that measured in the original 3D scene, a finding consistent with previous research showing that reducing depth cues significantly reduces the magnitude of size illusions[11]. (Note that the 16% reduction was measured under the same behavioral conditions as the original, brick hallway stimulus. During the fMRI conditions, which included a dynamic contrast-reversing stimulus and which required subjects to maintain fixation, most observers felt that the size illusion with the minimal depth cues was even weaker.) Consistent with the reduced perceptual effect, there was a reduced, though significant, fMRI difference (maximum response-curve distance = 15%, mean = 9%) with the back sphere activating a larger area in V1 than the front sphere (**Fig. 4c**).

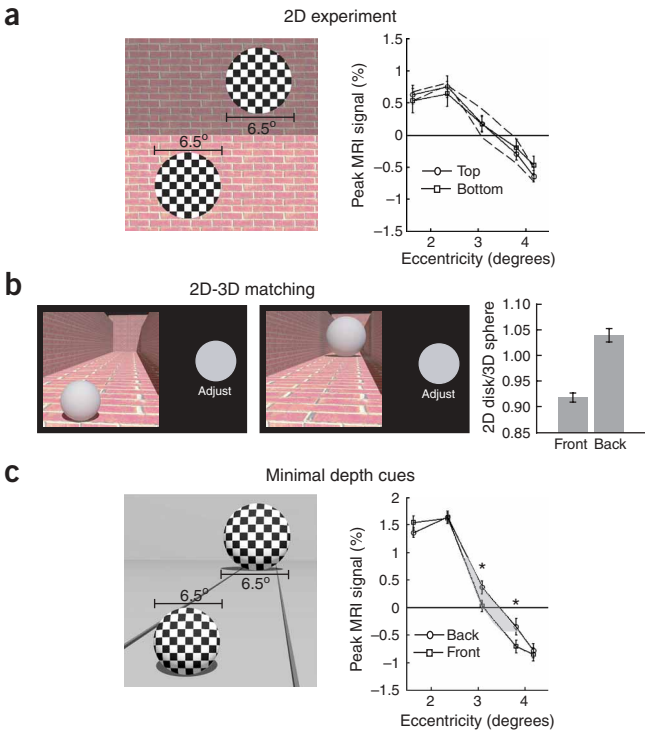

Figure 4 Control experiments. (**a**) A similar brick background pattern and luminance contrast, but no size illusion, was used. There was no difference in the measured signal as a function of eccentricity for the top (high contrast) versus bottom (low contrast) checkerboard locations. The dashed lines are the 3D data plotted from **Figure 3**. Note that the 2D response curves fall between the responses to the front and back spheres. (**b**) To directly compare 2D and 3D size judgments, a 2D disk located outside the 3D scene was adjusted to match the front and back spheres. The front and back spheres in the 3D scene were judged to be smaller and larger, respectively, than an equivalent 2D disk. (**c**) A 3D scene with minimal depth cues was used, resulting in a smaller perceptual effect than the original 3D scene. Consistent with the reduced perceptual effect, the fMRI effect was smaller, but still significant, with activity in response to the perceptually larger (back) sphere extending in eccentricity beyond that in response to the perceptually smaller (front) sphere. $*P < 0.05$. Error bars represent s.e.m.

DISCUSSION

We have demonstrated a relationship between the spatial extent of activation in human primary visual cortex and an object's perceived angular size. Previously it was assumed that retinotopic maps are fixed and solely reflect a feedforward mapping between the retina and cortex, such that when two images occupy the same portion of the visual field, they will activate the same cortical area. When the information to be represented is 2D (as in almost all previous retinotopic mapping studies), this characterization seems to be valid. But adding a third dimension to the information (such as exists in almost all naturally occurring stimuli) complicates this characterization. The ultimate goal of the visual system is clearly not to precisely measure the size of an image projected onto the retina. A more behaviorally critical property of an object is its size relative to the environment, which helps determine its identity and how one should interact with the object. Estimating an object's behaviorally relevant size requires that its retinal projection be scaled by its distance from the observer or from other objects in the environment. The results presented here indicate that the scaling process affects the retinotopic representation in V1, one of the earliest stages of the human visual system. On the basis of the current results, we suggest that the topographic representation in V1 should be thought of as dynamic and dependent on the 3D content in the scene. It remains to be seen, in future studies, what the limits of this rescaling process are as they relate to topographical changes in V1. For example, if a stimulus could be created that resulted in a doubling of perceived angular size, to what extent would this be reflected in topographic changes in V1? Presumably, feedforward inputs to V1 limit the degree of rescaling.

The source of the effect could arise from a number of different mechanisms. In our stimulus configuration, feedback from higher visual areas would seem to make an important contribution to the effect that we observed. Extracting depth information from the texture and perspective cues in our stimuli requires that the information be integrated over a large area and probably necessitates the large receptive fields found in higher-order visual areas. This depth information, once extracted, could then be used to rescale retinotopic representations in other visual areas. In addition, visual attention processes, which are known to be retinotopically specific[15–17], may make an important feedback contribution to the spatial extent of the response. However, it should be emphasized that an attention mechanism would require a redistribution of spatial attention in 2D (screen) coordinates based on 3D cues and not simply an attentional gain mechanism. Finally, as with any fMRI experiment, signal differences may not reflect differences in spiking in V1 neurons but could reflect differences in synaptic input. Overall, understanding the possible role of feedback and other mechanisms will require further experiments.

From our findings that perceptually larger stimuli result in an increased area of activation in V1, we can make a number of behavioral predictions. For example, previous detection and discrimination tasks that have depended on physical stimulus size (such as spatial summation; refs. 18,19) should have altered thresholds depending on perceived angular size. Previous psychophysical results are consistent with this prediction[20]. Similarly, an important question is whether there are resolution differences as a function of perceived size—a larger cortical representation may translate into improved spatial discrimination thresholds. Finally, visual aftereffects induced by adaptation may extend over a larger area in retinal space for stimuli perceived to be far away than for stimuli perceived to be close by.

Presumably, the visual system progressively transforms information from a retinal to an object-centered reference frame whereby retinal size is progressively removed from the representation. Thus, another important issue to address in future studies is the extent to which other retinotopic areas manifest a pattern of results similar to what we observed in V1. To make the necessary measurements in intermediate retinotopic areas (V2, V3, V4 and so on), however, will require the use of an imaging protocol with greater spatial resolution. Extrastriate retinotopic areas become progressively smaller and, even with our current imaging parameters, we could not differentiate ROIs in V2 with sufficient resolution to perform a similar analysis.

Our results are not consistent with a previous neuroimaging experiment that used a spatial position illusion[21]. In that study, stationary patterns containing inward and outward moving elements created the perception of an inward and outward position shift of the elements. Thus, the stimulus with the outward moving elements appeared to occupy a larger portion of the visual field than the stimulus with inward moving elements. Paradoxically, the study found a relative increase in the fMRI signal in eccentric V1 for the inward (smaller) moving patterns and a relative increase in foveal V1 for outward (larger) moving patterns. Additional stimulus conditions in the original study as well as replication studies performed by another laboratory

(J. Liu, D. Ress, S. Nakadomari & B.A. Wandell, *Soc. Neurosci. Abstr.* 18.11, 2004) indicate that changes in perceived position are irrelevant to the effect. Instead, the source of the fMRI differences seems to be a large motion signal associated with the trailing edge of the stimuli, changes in motion direction or both. Given that the changes in activity distribution we observed were relatively small, it is likely that if present in this earlier study[21], they were dominated by the large motion signal and were thus not measurable with fMRI.

Our results are consistent with earlier work suggesting that neural responses in early visual cortex may change as a function of depth to allow for object scaling[20,22–25], pointing to a variety of ways in which neural processing could be modified in V1. Some of this previous work has identified changes in firing rate as a function of distance ('distance tuning', ref. 25) whereas other research has suggested that receptive fields may change size as a function of distance to the object[20,22,23]. Computational models have also identified strategies for dynamic control of information between arrays of neurons at different levels of the visual pathway, which allow for shifts in the relative alignment of inputs and outputs[26]. Although the specific mechanisms underlying the effects that we measured remain unidentified, our results demonstrate a previously unknown correspondence between perceived size and retinotopic maps in human primary visual cortex.

METHODS

Participants. Five volunteers with normal or corrected-to-normal vision participated in 1–3 fMRI imaging sessions each. All subjects who participated in the fMRI experiments also participated in the behavioral sessions. Informed consent was obtained according to procedures approved by the University of Minnesota Internal Review Board.

Visual stimuli. All stimuli (except the disks used in Experiment 1) were rendered using the Radiance software package[27] and were viewed binocularly (see **Supplementary Note** online for a discussion of binocular viewing and vergence eye movements and their relationship to our results). The scene was illuminated by a mixture of diffuse and single distant punctate light-source, both of which were neutral in chromaticity. We wrote the software for the behavioral experiments using the Java programming platform (http://java.sun.com). In the fMRI experiment, identical background images were used for the counterphase stimulus presentations to ensure that there were no slight pixel modulations in the background caused by differences in rendering between the two counterphase spheres. The entire scene occupied 18° of visual angle. Stimuli were projected using an LCD projector (Sharp) onto a rear-projection screen located in the magnet bore and were viewed with an angled mirror. During scanning, we used Presentation software (http://www.neurobehavioralsystems.com) to display the stimuli, which were synchronized with MRI data acquisition. Subjects were instructed to maintain fixation on a small point that moved between presentation locations throughout the experiment.

Behavioral experiment. Two behavioral measurements were made while subjects were positioned in the MRI scanner. (Subjects performed additional trials, with different measurement techniques, outside the scanner. We obtained the same pattern of results, some of which are described in the **Supplementary Methods**.) The experiments were designed to establish the lower bound of the magnitude of the size illusion. Subjects were given unlimited time to inspect the scene and were free to move their eyes and scan the stimuli during inspection. For the first experiment, subjects were presented with the 3D scene and both spheres and were asked to adjust the size of the front sphere until its angular size matched that of the back sphere. The concept of 'angular size' was carefully explained and subjects were told to adjust the size so that the two images of the spheres would perfectly overlap if moved to the same location on the screen. (Because head position was fixed with respect to the stimulus, the number of pixels an object occupies on the screen, the 'image size', was also used to describe the task.) The behavioral effect was quantified by computing the ratio of the size of the front sphere to the size of the back sphere. The second experiment was similar to the first, except that a single sphere was presented and subjects adjusted a 2D gray disk located outside the scene until it matched the sphere in angular size. The behavioral effect was quantified by dividing the size of the 2D disk adjusted to match the back sphere by the size of the back sphere and by dividing the size of the 2D disk adjusted to match the front sphere by the size of the front sphere. For both experiments, each measurement consisted of five trials. Behavioral data were also collected with either a static or a counterphase-flickering checkerboard texture added to the spheres. Overall, these measurements did not differ from those obtained using static, gray spheres. However, in preliminary testing, one subject was able to use a matching strategy based purely on the apparent size of the checks in the checkerboard textures. We used gray spheres for all subjects to eliminate the possible use of this strategy.

fMRI procedure. MRI data were collected on a 3-T scanner (Siemens Trio) outfitted with an eight-channel phase-array coil. Echoplanar data were acquired using standard parameters (24 3-mm-thick axial slices; field of view, 220 mm; matrix, 64 × 64; repetition time (TR), 2.0 s; echo time (TE), 30 ms; flip angle, 70°). We acquired 8–12 functional runs, each consisting of 104 images, for every subject. The first four volumes were discarded to allow for magnetization equilibration. A T1-weighted anatomical volume (3D MPRAGE; 1 × 1 × 1 mm^3 resolution) was acquired for localization and visualization of the functional data.

After motion correction (SPM99, http://www.fil.ion.ucl.ac.uk/spm), the functional data were coregistered with the anatomical scan. Data were analyzed in equally sized, predefined ROIs in V1, averaging four functional voxels per ROI. Maps of the horizontal and vertical meridian (10-s block design alternating between horizontal and vertical meridian stimuli) identified the border of V1 and V2. A series of counterphase-flickering annuli (10-s block design alternating between annuli of different radii) were used to define regions within V1 corresponding to five eccentricities along the radius of the spheres (3D experiment) and disks (2D experiment). The ROIs were defined using BrainVoyager and visualized on inflated cortices for each subject. Time courses from each ROI were then extracted and imported into Matlab for further analyses. This included an event-related averaging of each stimulus condition (with the average of the last two time points of each fixation condition serving as a baseline for each stimulus block) and extraction of peak responses by averaging time points 6–10 s after the start of a presentation block for each stimulus condition. Statistical paired *t*-tests were used to evaluate differences in the peak response for each of the ROIs.

We estimated the difference in the peak response curves using two different methods. The first estimated the 'effect size'. We wanted to estimate how much further one curve extended beyond another in eccentricity and to express this difference as a percentage. This was done to compare the fMRI data to behavioral measures of the perceptual effect size (also expressed as percentages). We estimated the percentage difference between peak response curves by first performing a bicubic interpolation to obtain a denser sampling of the curves. Next, we calculated the percentage difference in eccentricity between the curves at 20 equally spaced intervals between the half-maximum and half-minimum point of the response curves. This range was found to consistently capture the maximum differences in the curves.

The second method for characterizing the peak response curves estimated the absolute 2D eccentricities activated by the 3D (sphere) stimuli. We wanted to estimate how many degrees of 2D visual angle in cortex were activated by the near and far 3D stimuli. This involved establishing a criterion for deciding where in the cortex activation ends. To do this, we considered the 6.5° curves in both of the 2D experiments (**Fig. 3**, middle and bottom rows), as the spheres in the 3D room were also 6.5°. This also allowed us a replication opportunity, as the 2D 6.5° curves were measured twice. We found that when the curves reached the 3.25° eccentricity point (that is, the radius of the 6.5° disk), the curves were at 23% (**Fig. 3**, middle row) and 21% (**Fig. 3**, bottom row) of their maximum value. To estimate the absolute 2D eccentricities activated by the 3D stimuli, we obtained the eccentricity value that corresponded to the 3D stimulus curves when they reached 22% of their maximum value.

Note: Supplementary information is available on the Nature Neuroscience website.

ACKNOWLEDGMENTS

We thank S. He, F. Fang and P. Sinha for their comments and suggestions related to this manuscript. This work was supported by the US National Institutes of

Health (F32 EY015342 to S.O.M. and RO1 EY-015261 to D.K.) and the National Geo-Spatial Intelligence Agency (HM1582-05-C-0003 to S.O.M.).

COMPETING INTERESTS STATEMENT

The authors declare that they have no competing financial interests.

Published online at http://www.nature.com/natureneuroscience/
Reprints and permissions information is available online at http://npg.nature.com/reprintsandpermissions/

1. Holway, A.H. & Boring, E.G. Determinants of apparent visual size with distance variant. *Am. J. Psychol.* **54**, 21–37 (1941).
2. Joynson, R.B. The problem of size and distance. *Q. J. Exp. Psychol.* **1**, 119–135 (1949).
3. Gilinsky, A.S. The effect of attitude upon the perception of size. *Am. J. Psychol.* **68**, 173–192 (1955).
4. Ono, H. Distal and proximal size under reduced and non-reduced viewing conditions. *Am. J. Psychol.* **79**, 234–241 (1966).
5. Kaufman, L. & Rock, I. The moon illusion, I. *Science* **136**, 953–961 (1962).
6. King, W.L. & Gruber, H.E. Moon illusion & Emmert's law. *Science* **135**, 1125–1126 (1962).
7. Rock, I. & Kaufman, L. The moon illusion, II. *Science* **136**, 1023–1031 (1962).
8. Kaufman, L. & Kaufman, J.H. Explaining the moon illusion. *Proc. Natl. Acad. Sci. USA* **97**, 500–505 (2000).
9. Foley, J.M. The size-distance relation and intrinsic geometry of visual space: implications for processing. *Vision Res.* **12**, 323–332 (1972).
10. Jenkin, N. & Hyman, R. Attitude and distance-estimation as variables in size-matching. *Am. J. Psychol.* **72**, 68–76 (1959).
11. Leibowitz, H., Brislin, R., Perlmutter, L. & Hennessy, R. Ponzo perspective illusion as a manifestation of space perception. *Science* **166**, 1174–1176 (1969).
12. McCready, D. On size, distance, and visual angle perception. *Percept. Psychophys.* **37**, 323–334 (1985).
13. Engel, S.A., Glover, G.H. & Wandell, B.A. Retinotopic organization in human visual cortex and the spatial precision of functional MRI. *Cereb. Cortex* **7**, 181–192 (1997).
14. Sereno, M.I. *et al.* Borders of multiple visual areas in humans revealed by functional magnetic resonance imaging. *Science* **268**, 889–893 (1995).
15. Tootell, R.B. *et al.* The retinotopy of visual spatial attention. *Neuron* **21**, 1409–1422 (1998).
16. Somers, D.C., Dale, A.M., Seiffert, A.E. & Tootell, R.B. Functional MRI reveals spatially specific attentional modulation in human primary visual cortex. *Proc. Natl. Acad. Sci. USA* **96**, 1663–1668 (1999).
17. Ress, D., Backus, B.T. & Heeger, D.J. Activity in primary visual cortex predicts performance in a visual detection task. *Nat. Neurosci.* **3**, 940–945 (2000).
18. Barlow, H. Temporal and spatial summation in human vision at different background intensities. *J. Physiol. (Lond.)* **141**, 337–350 (1958).
19. Kersten, D. Spatial summation in visual noise. *Vision Res.* **24**, 1977–1990 (1984).
20. Richards, W. Apparent modifiability of receptive fields during accommodation and convergence and a model for size constancy. *Neuropsychologia* **5**, 63–72 (1967).
21. Whitney, D. *et al.* Flexible retinotopy: motion-dependent position coding in the visual cortex. *Science* **302**, 878–881 (2003).
22. Richards, W. Spatial remapping in the primate visual system. *Kybernetik* **4**, 146–156 (1968).
23. Marg, E. & Adams, J.E. Evidence for a neurological zoom system in vision from angular changes in some receptive fields of single neurons with changes in fixation distance in the human visual cortex. *Experientia* **26**, 270–271 (1970).
24. Trotter, Y., Celebrini, S., Stricanne, B., Thorpe, S. & Imbert, M. Modulation of neural stereoscopic processing in primate area V1 by the viewing distance. *Science* **257**, 1279–1281 (1992).
25. Dobbins, A.C., Jeo, R.M., Fiser, J. & Allman, J.M. Distance modulation of neural activity in the visual cortex. *Science* **281**, 552–555 (1998).
26. Anderson, C.H. & Van Essen, D.C. Shifter circuits: a computational strategy for dynamic aspects of visual processing. *Proc. Natl. Acad. Sci. USA* **84**, 6297–6301 (1987).
27. Larson, G.W. & Shakespeare, R. *Rendering with Radiance: the Art and Science of Lighting and Visualization* (Morgan Kaufmann, San Francisco, 1996).

2. Stephan, F.K. & Zucker, I. *Proc. Natl. Acad. Sci. USA* **69**, 1583–1586 (1972).
3. Moore, R.Y. & Eichler, V.B. *Brain Res.* **42**, 201–206 (1972).
4. Hastings, M.H. & Herzog, E.D. *J. Biol. Rhythms* **19**, 400–413 (2004).
5. Richter, C.P. *Comp. Psychol. Monogr.* **1**, 1–54 (1922).
6. Krieger, D.T., Hauser, H. & Krey, L.C. *Science* **197**, 398–399 (1977).
7. Stephan, F.K. *J. Biol. Rhythms* **17**, 284–292 (2002).
8. Schibler, U., Ripperger, J. & Brown, S.A. *J. Biol. Rhythms* **18**, 250–260 (2003).
9. Davidson, A.J., Cappendijk, S.L. & Stephan, F.K. *Am. J. Physiol. Regul. Integr. Comp. Physiol.* **278**, R1296–R1304 (2000).
10. Yamazaki, S., Kerbeshian, M.C., Hocker, C.G., Block, G.D. & Menaker, M. *J. Neurosci.* **18**, 10709–10723 (1998).
11. Stokkan, K.A., Yamazaki, S., Tei, H., Sakaki, Y. & Menaker, M. *Science* **291**, 490–493 (2001).
12. Granados-Fuentes, D., Saxena, M.T., Prolo, L.M., Aton, S.J. & Herzog, E.D. *Eur. J. Neurosci.* **19**, 898–906 (2004).
13. Landry, G.J., Simon, M.M., Webb, I.C. & Mistlberger, R.E. *Am. J. Physiol. Regul. Integr. Comp. Physiol.* published online, January 19 2006 (PMID: 16424080) (2006).
14. Akiyama, M. *et al. Eur. J. Neurosci.* **20**, 3054–3062 (2004).
15. Mieda, M. *et al. J. Neurosci.* **24**, 10493–10501 (2004).

Total recall

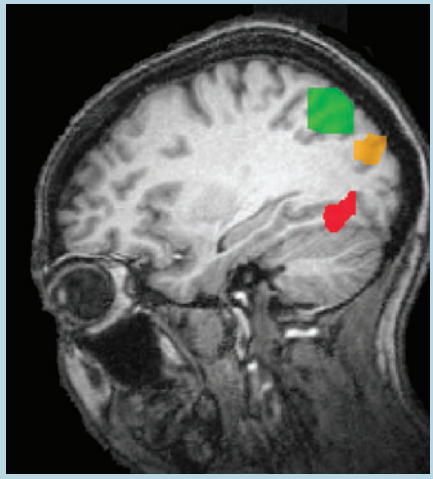

The importance of visual short-term memory is clear to anyone who has ever played the children's card game that requires players to identify identical face-down cards at different locations. Visual short-term memory is the temporary buffer that stores visual information. Behavioral studies indicate that this buffer can store up to four objects, but more recent evidence indicates that the maximum number of objects that can be stored becomes smaller as object complexity increases. It is therefore unclear whether visual short-term memory capacity is limited to a fixed number of objects or if it is variable.

In a paper in *Nature* ('Dissociable neural mechanisms supporting visual short-term memory for objects', doi:10.1038/nature04262), Yaoda Xu and Marvin Chun resolve this controversy by using functional magnetic resonance imaging (fMRI) to dissociate object representations in parietal and occipital cortices. Observers were asked to detect a change in a simple or complex shape feature in the same set of objects. The number of objects in a set was varied. Observers did better when they had to detect a change in a simple feature and also when the number of objects was small. The authors found a similar interaction in the superior intraparietal sulcus (green in the picture) and the lateral occipital cortex (red), which tracked behavioral performance, but only for simple shape features, not complex ones. In contrast, activation in the inferior parietal sulcus (orange) tracked overall performance based only on the number of objects seen, regardless of whether observers judged simple or complex shape features. In control experiments, the authors ruled out perceptual processing limitations and spatial location as an explanation for these results, and also correlated the observed activity with the encoding and maintenance phases of visual short-term memory.

These results indicate that there are differing representations for visual short-term memory in the brain. Whereas the inferior parietal sulcus representation is fixed by the number of objects, object representation in the superior parietal sulcus and the lateral occipital cortex varies according to the complexity of the objects being held in visual short-term memory. The inferior parietal sulcus representation is thus likely to be the mechanism determining the maximum number of objects that can be held in visual short-term memory and may determine capacity limitations in tasks such as subitizing and multiple object tracking. The superior parietal sulcus and lateral occipital cortex representation are more likely to contain detailed representations of objects. These results demonstrate that visual short-term memory capacity is determined both by object number and by object complexity.

Charvy Narain

Perceived size matters

Philipp Sterzer & Geraint Rees

Activity in early visual processing areas is often thought to reflect physical input from the retina, rather than conscious perception. A new study now finds that activity in V1 corresponds to perceived rather than actual object size.

Try this quick do-it-yourself experiment: look at an illuminated light bulb for a few seconds and then view the afterimage on your hand and finally on a nearby wall. The afterimage seems bigger as the surface on which it is viewed becomes farther away. This illusion[1], reported by Emmert over one hundred years ago, demonstrates one of the most intriguing aspects of vision: even when objects cast exactly the same size pattern of light on the retina, they appear to be markedly different in size when viewed at different distances. In going from retinal image to conscious perception, the visual system is therefore able to factor in perceived distance to change how big something looks.

Exactly how the visual system achieves this feat remains unclear. It was traditionally assumed that early visual processing areas primarily reflect the physical input from the retina, whereas activity in higher-order areas more closely resembles conscious perception. Such an account would hold that the perceived size of an object would more closely match activity in higher visual

The authors are in the Wellcome Department of Imaging Neuroscience, Institute of Neurology, University College London, 12 Queen Square, London WC1N 3BG, UK and at the Institute of Cognitive Neuroscience, University College London, 17 Queen Square, London WC1N 3AR, UK.
e-mail: g.rees@fil.ion.ucl.ac.uk

areas. However, in this issue, Murray and colleagues[2] find a very different pattern of results. They used functional magnetic resonance imaging (MRI) to measure the spatial pattern of activity in human primary visual cortex (V1) while volunteers viewed objects that were physically the same size (and therefore produced identical patterns of retinal input) but were perceived as different in size. Surprisingly, the spatial extent of activity in the very first cortical visual area (V1) reflected not the size of the retinal input, but instead the perceived size of the object. This remarkable finding challenges our notion that V1 contains a very precise one-to-one map of retinal input, and for the first time provides a link between the spatial extent of what we perceive and the exact spatial distribution of activity in human V1.

The authors measured brain activity while subjects viewed pictures of identically sized spheres placed in a picture of a three-dimensional (3D) hallway. A compelling size illusion is immediately apparent (**Fig. 1**); the sphere at the end of the hallway looks markedly bigger than the one at the start, even though the actual size of the two spheres is exactly the same. Indeed, when subjects were asked to compare the size of these objects with two-dimensional (2D) flat disks (presented on a background without 3D cues), they judged the front sphere to be slightly smaller than the equally sized 2D disk and the back sphere to be larger. The contextual cues to depth in the 3D scene (textural gradients and linear perspective) affect the perceived size of the objects.

Using retinotopic mapping to delineate primary visual cortex, Murray and colleagues examined whether the size of activation patterns in V1 differed when subjects looked at either the front or back spheres. Remarkably, when the sphere that subjects were looking at was perceived to be bigger (due to the contextual cues), activity in V1 spread over a larger area than when it was perceived to be smaller, even though the size of the retinal image produced by the spheres was identical. Activity at the earliest stages of cortical processing does not therefore simply reflect the pattern of light falling on the retina. Somehow the complex three-dimensional cues present in the scene (**Fig. 1**) can be integrated to take into account perceived depth in the representation present in V1.

As V1 is a relatively large cortical area relative to the spatial resolution of functional MRI, Murray and colleagues were able to compare in detail the size of the activation produced by purely perceptual (illusory) variations in object size and physical changes in object size. They compared the difference in the distribution of V1 activity between the perceptually 'bigger' and 'smaller' spheres (**Fig. 1**) with that between two-dimensional discs that physically matched the perceived size difference. They found strikingly similar differences in V1 activity patterns in each case, suggesting that differences in perceived size (rather than retinal input) matter for V1. This further strengthens the claim that the V1 representation of an object closely reflects its perceived size. In other careful control experiments, Murray and colleagues ruled out other possible explanations, such as the local contextual cues altering perceived brightness (which can potentially affect V1 activation[3]) rather than just perceived size.

Murray and colleagues could not determine precisely where this effect of perceived size on V1 activity arises because they could not examine activity beyond V1 for technical reasons. The visual system must combine information about the perceived depth of an object (provided by the environmental context in **Fig. 1**) with the projection of that object on the retina. Computing perceived depth from two-dimensional pictorial cues such as linear perspective and texture gradients is associated with activity in parietal cortex[4,5]. Presumably, such signals reflecting perceived depth can influence V1 through feedback signals that influence the size of the object representation. However, whether the object representation in V1 causes the conscious perception of size remains an open question. Intriguingly, the perceived size of afterimages generated by stimulating the blind hemifield of an individual whose primary visual cortex has been surgically removed nevertheless obeys Emmert's law[6]. This suggests that activity in areas other than V1 may be sufficient to support scaling of perceived size for at least some types of image with perceived distance. A closer characterization of the functional role of V1 in the conscious perception of size therefore remains an intriguing topic for future research.

This work is not the first to show that V1 activity can be strongly linked to conscious perception rather than to physical (retinal) stimulation[7]. It is also clear that neural processing in V1 reflects not just feed-forward signals but also feedback influences from higher areas[8]. However, this work not only provides a particularly clear and compelling example of these properties but also, for the first time, clearly links the spatial extent of what we perceive (rather than, for example, contrast or direction of motion) to the spatial extent of activity in V1. More

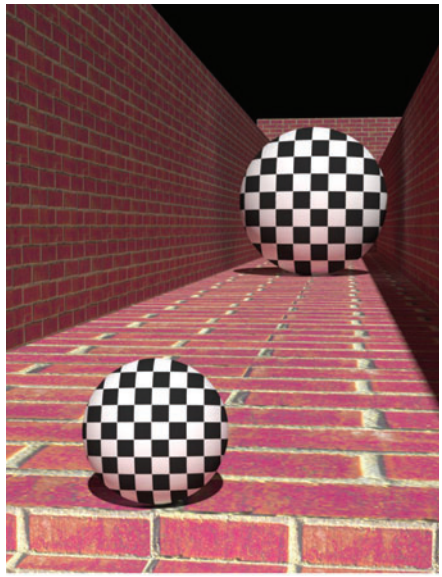

Scott Murray

Figure 1 A color picture of the stimuli used in the experiment. The two spheres are actually the same size.

fundamentally, these findings force us to re-evaluate the notion of a 'hard-wired' retinotopy in V1. The finding that V1 contains a topographic map of the retinal projection of the visual field has been central to visual neuroscience[9,10]. Instead it now seems that the topographic map in V1 can be modified dynamically according to the perceived size of an object. This has important implications not only for understanding the role of V1 in visual processing but also in practical terms. For instance, it has become common practice in functional MRI studies focusing on early visual areas to functionally localize spatially delimited regions of interest using retinotopic mapping. The general usefulness of this approach notwithstanding, future studies will have to take into account the possibility that visual context can dynamically modify this retinotopy, even in early visual areas.

Dynamic shifts in how retinal outputs map onto cortical targets (such as the retinotopic maps in V1) are a key component of an influential computational model[11] that seeks to resolve computational problems in the domains of stereopsis (depth perception from binocular cues), spatial attention and motion perception. Thus, flexible mappings between arrays of neurons at different levels of the visual pathway may reflect a common computational strategy for optimal vision. The limits of this 'flexible retinotopy' (ref. 12) will need to be probed and the fine-grained neural mechanisms uncovered through complementary studies

in nonhuman primates. At a single neuron level, primate V1 responses show signals that change according to the distance of an object[13,14], forming a potential neural substrate for the dynamic changes observed at a much coarser spatial scale by Murray and colleagues.

Indeed, at a fine-grained level, their findings also raise intriguing questions about whether a V1 representation of the environment that reflects perceived depth and size can be internally coherent. For example, when two objects at different perceived depths partially occlude each other, correct border assignments may be particularly complex as portions of the objects adjacent to the border may be relatively displaced according to perceived depth. The current observation that the near and far objects were judged to appear both smaller and larger with respect to an equivalently sized two-dimensional object may suggest a 'push-pull' mechanism for maintaining coherence in a spatially distributed V1 representation of the subjects perceptions.

Taken together, these compelling findings force us once again to consider a revised model of visual processing in which V1, far from being a passive feed-forward recipient of retinal signals, instead flexibly combines retinal and extraretinal signals to potentially build an integrated representation of the perceived visual environment. Future study of how V1 activity relates to human consciousness will doubtless continue to be both interesting and informative.

1. Emmert, E. *Klin. Mbl. Augenheilk.* **19**, 443–450 (1881).
2. Murray, S.O., Boyaci, H. & Kersten, D. *Nat. Neurosci.* **9**, 429–434 (2006).
3. Haynes, J.D., Lotto, R.B. & Rees, G. *Proc. Natl. Acad. Sci. USA* **101**, 4286–4291 (2004).
4. Shikata, E. *et al. J. Neurophysiol.* **85**, 1309–1314 (2001).
5. Tsutsui, K., Sakata, H., Naganuma, T. & Taira, M. *Science* **298**, 409–412 (2002).
6. Weiskrantz, L., Cowey, A. & Hodinott-Hill, I. *Nat. Neurosci.* **5**, 101–102 (2002).
7. Tong, F. *Nat. Rev. Neurosci.* **4**, 219–229 (2003).
8. Hupe, J.M. *et al. Nature* **394**, 784–787 (1998).
9. Glickstein, M. & Whitteridge, D. *Trends Neurosci.* **10**, 350–353 (1987).
10. Holmes, G. *Br. J. Ophthalmol.* **2**, 353–384 (1918).
11. Anderson D.H. & van Essen D.C. *Proc. Natl. Acad. Sci. USA* **84**, 6297–6301 (1987).
12. Whitney, D. *et al. Science* **302**, 878–881 (2003).
13. Dobbins, A.C., Jeo, R.M., Fiser, J. & Allman, J.M. *Science* **281**, 552–555 (1998).
14. Trotter, Y., Celebrini, S., Stricanne, B., Thorpe, S. & Imbert, M. *Science* **257**, 1279–1281 (1992).

Quantifying motor neuron loss in ALS

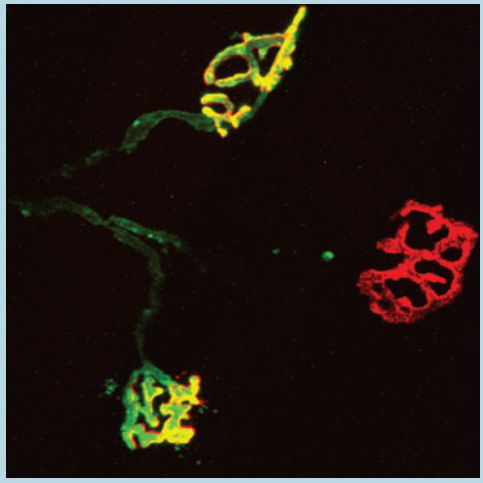

Amyotrophic lateral sclerosis (ALS or Lou Gehrig's disease) leads to paralysis from the death of motor neurons in the spinal cord and brainstem. It is incurable, and patients typically die within three to five years of disease onset. Neurodegenerative diseases like ALS can progress slowly, with years of clinically undetectable symptoms followed by rapid deterioration. Although ALS selectively targets motor neurons, it has remained unclear whether particular synapses are selectively targeted and whether these synapses are lost gradually or abruptly.

In an article in this issue (page 408), Pico Caroni and colleagues addressed this issue by creating a quantitative map of the innervation of hindlimb muscle compartments by motor neurons in the mouse. They then went on to study the mechanisms of early disease progression in a mouse model of ALS.

Motor neurons innervating skeletal muscle fibers are subdivided into three functional subtypes—fast twitch and fast fatiguable (FF), fast twitch and fatigue resistant (FR) and slow twitch (S). The authors used transgenic mice expressing green fluorescent protein in only a few neurons and mapped the distribution of all synapses made by individual motor neurons in the lateral gastrocnemius muscle. Once they created a topographic map of motor neuron innervation, they analyzed denervation patterns in mice containing a mutation in the enzyme superoxide dismutase (SOD1). In this familial ALS mouse model, they found that FF axons were selectively affected early on in the disease and that these abruptly disconnected from their peripheral synapses when the mice were 48–52 days old. FR motor neurons innervating the same muscle compartments compensated initially for this loss by reinnervating neuromuscular junctions (NMJs) on the muscle fibers, but over time, were less able to maintain the additional NMJs. They then started pruning their nerve branches by the time the mice were 80–90 days old. S-type motor neurons were particularly resistant to disease, and maintained expanded motor units up to the time the mice died.

What makes the FF and FR motor neuron axons selectively vulnerable to disease? The authors did cross-innervation experiments and nerve crush studies and concluded that the early vulnerability of FF motor neurons reflects a vulnerability of the presynaptic motor neuron axon rather than its target muscle or peripheral synapses. They also found that axonal transport was particularly vulnerable in FF and to a lesser degree in FR axons, leading to synaptic vesicle stalling and loss from NMJs. In the figure, the NMJ in the center has lost all synaptic signal (green, synaptic vesicle marker SV2; red, acetylcholine receptor) but is still innervated. Other NMJs may be less affected, like the lower one in the figure. Daily applications of the growth factor ciliary neurotrophic factor (CNTF) protected FF axons from synaptic vesicle loss and peripheral pruning and also helped to maintain the expanded size and innervation of compensating FR motor neuron axons. CNTF helped to boost axonal resistance to disease by causing neurofilament density reductions in both FF and FR neurons and by preventing the upregulation of an anti-apoptotic protein, Bc12a1-a, in motor neurons.

By providing a quantitative account of the selective vulnerability of different motor neuron populations during the progression of disease, this work opens up new possibilities for treating ALS and related motor neuron disorders.

Kalyani Narasimhan